Correlations between the nuclear matter symmetry energy, its slope, and curvature from a nonrelativistic solvable approach and beyond

B. M. Santos,[1] M. Dutra,[2] O. Lourenço,[3] and A. Delfino[1]

[1]*Instituto de Física, Universidade Federal Fluminense, 24210-150 Niterói, RJ, Brazil*

[2]*Departamento de Física e Matemática—ICT, Universidade Federal Fluminense, 28895-532 Rio das Ostras, RJ, Brazil*

[3]*Departamento de Ciências da Natureza, Matemática e Educação, CCA, Universidade Federal de São Carlos, 13600-970 Araras, SP, Brazil*

(Received 26 May 2014; revised manuscript received 28 July 2014; published 15 September 2014)

By using point-coupling versions of finite-range nuclear relativistic mean-field models containing cubic and quartic self-interactions in the scalar field σ, a nonrelativistic limit is achieved. This approach allows an analytical expression for the symmetry energy (J) as a function of its slope (L) in a unified form, namely, $L = 3J + f(m^*, \rho_o, B_o, K_o)$, where the quantities m^*, ρ_o, B_o, and K_o are bulk parameters at the nuclear matter saturation density ρ_o. This result establishes a linear correlation between L and J which is reinforced by exact relativistic calculations. An analogous analytical correlation is also found for J, L, and the symmetry energy curvature ($K_{\rm sym}$). Based on these results, we propose graphic constraints in $L \times J$ and $K_{\rm sym} \times L$ planes that finite-range models must satisfy.

DOI: 10.1103/PhysRevC.90.035203 PACS number(s): 21.65.Mn, 13.75.Cs, 21.30.Fe, 21.60.−n

I. INTRODUCTION

Several bulk parameter quantities help our understanding of nuclear matter properties. One of them is the symmetry energy $\mathcal{S}$, which can be expanded as a function of the nuclear density ρ as $\mathcal{S}(\rho) = J + Lx + \frac{1}{2}K_{\rm sym}x^2 + \frac{1}{6}Q_{\rm sym}x^3 + O(x^4)$, where $x = (\rho - \rho_o)/3\rho_o$ and ρ_o is the nuclear matter saturation density. The coefficients of this expansion, namely, J, L, $K_{\rm sym}$, and $Q_{\rm sym}$ are, respectively, the symmetry energy at the saturation density, the slope, the curvature, and the third derivative (skewness) of $\mathcal{S}$, all of them also evaluated at $\rho = \rho_o$. The symmetry energy is important for modeling nuclear matter and finite nuclei by probing the isospin part of nuclear interactions. Particularly, it is also important in different issues of astrophysics [1,2]. For a study of the effects of J and L on neutron star properties such as the minimum mass that enables the Urca effect, see, for instance, Ref. [3].

A compelling feature of nuclear matter bulk parameter studies has been the investigation of correlations among them. The investigation of correlations between observables is an important issue in physics since knowledge of one observable may carry information about the other. In nuclear physics, particularly, the exact nucleon-nucleon interaction is unknown, so different proposals for nuclear forces are used. Usually, the free parameters of nuclear models are eliminated in favor of a set of observables. Therefore, in nuclear physics, correlations between two observables acquire an enormous importance because they reduce the set of independent relevant quantities to be used in the construction of nuclear models, avoiding redundant free-parameter fittings [4]. There are few well-established correlations between nuclear bulk parameters. One of them, usually known as the Coester line [5], correlates ρ_o and the nuclear matter binding energy B_o. Another one was studied by Furnstahl-Rusnak-Serot (FRS) [6] and involves the correlation between the finite nuclei spin-orbit splittings and the ratio $m^* = M_o^*/M$ for a family of effective finite-range (FR) relativistic mean-field (RMF) models. Here M_o^* is the Dirac effective mass of the nucleon in symmetric nuclear matter at $\rho = \rho_o$. The results show that good values for these splittings are obtained by a restricted class of FR models that present m^* in a range of $0.58 \leqslant m^* \leqslant 0.64$. Hereafter, we will refer to this range as the FRS constraint. Recently, a correlation between L and J has been verified by Ducoin *et al.* [7] for a set of effective relativistic and nonrelativistic nuclear models. Such a study was based on numerical results for J and L, obtained from different parametrizations. We also call the readers attention to previous investigations on analytical expressions for J and L in relativistic and nonrelativistic many-nucleon models in Refs. [8,9].

Theoretically, J and L are expected to be constrained [10,11]. Nevertheless, no analytical relationship between these quantities is known up to now. That is why we find it important to have a way to relate the two quantities analytically. In order to proceed in this direction in our paper, we have chosen to follow three steps to simplify the FR models which parametrize the infinite nuclear matter bulk parameters and finite nuclei properties [12–14]. First, we select FR models containing cubic and quartic interactions in the scalar field σ; i.e., we choose models with σ^3 and σ^4 contributions in their Lagrangian density. Basically, they are known as Boguta-Bodmer models [15]. Second, we use their point-coupling versions [16–21]. We need to emphasize here that the point-coupling models are as good as the FR ones in the description of nuclear matter and finite nuclei. For instance, in Ref. [21], the authors were able to obtain, by using a relativistic zero-range model, ground-state binding energies, spin-orbit splittings, and rms charge radii of a large set of closed shell nuclei, as well as of nuclei outside the valley of β stability (see their Tables VIII and X), clearly showing the success of these kinds of model. As a side remark, we note that the linear point-coupling model and the Walecka one are exactly the same, as one can see in Ref. [22]. Third, we perform a nonrelativistic (NR) limit of the point-coupling models, based on normalized spinor wave functions after small component

reduction, exactly in the same way as developed in Ref. [23]. Such a procedure was already used in Ref. [24], in which very good results were found for $\rho \leqslant \rho_o$.

Following these steps, we were able to write, in an analytical way, L and $K_{\rm sym}$ as a function of ρ_o, B_o, m^*, and K_o (incompressibility at the saturation density). Our results indicate that both approaches, namely, the NR limit and the FR-RMF models, suggest a decreasing L when m^* increases whereas the L dependence on K_o is very weak. Similar behavior is also found regarding the m^* and K_o dependence of $K_{\rm sym}$. In the case of symmetry energy slope, we also could predict a linear correlation between L and J, which was also supported by the exact FR-RMF calculations.

In particular cases (models presenting close values for K_o), our NR calculations also indicate another linear correlation for two distinct cases, namely, (i) between $K_{\rm sym}$ and L for fixed values of J or (ii) between $K_{\rm sym}$ and J for fixed values of L. These results are also confirmed by the relativistic models submitted to the same conditions.

Our paper is organized as follows. In Sec. II, we obtain the expressions for J and L for the NR limit of the point-coupling models, and we show how they are correlated with each other. In Sec. III, we present, based on these correlations, the predictions on the exact FR-RMF models, also proposing new constraints that such models should satisfy in order to exhibit good values for finite nuclei spin-orbit splittings. Finally, in Sec. IV, the main conclusions are summarized.

II. THE NONRELATIVISTIC LIMIT OF NONLINEAR POINT-COUPLING MODELS

The relativistic nonlinear point-coupling (NLPC) versions of the Boguta-Bodmer models are described by the following Lagrangian density:

$$\begin{aligned}\mathcal{L}_{\rm NLPC} = {}& \bar{\psi}(i\gamma^\mu\partial_\mu - M)\psi - \frac{1}{2}G_{\rm V}^2(\bar{\psi}\gamma^\mu\psi)^2 \\ & + \frac{1}{2}G_{\rm S}^2(\bar{\psi}\psi)^2 + \frac{A}{3}(\bar{\psi}\psi)^3 + \frac{B}{4}(\bar{\psi}\psi)^4 \\ & - \frac{1}{2}G_{\rm TV}^2(\bar{\psi}\gamma^\mu\vec{\tau}\psi)^2, \end{aligned} \tag{1}$$

which mimics the two-, three-, and four-body pointlike interactions with the fermionic spinor field ψ associated with the nucleon of mass M. In this equation, the last term was included in order to take into account the asymmetry of the system (different number of protons and neutrons). In the nonrelativistic limit of the NLPC model, and by using the mean-field approach, the energy density functional at zero temperature for asymmetric nuclear matter is written as

$$\begin{aligned}\varepsilon^{\rm (NR)}(\rho,y) = {}& \left(G_{\rm V}^2 - G_{\rm S}^2\right)\rho^2 - A\rho^3 - B\rho^4 \\ & + G_{\rm TV}^2\rho^2(2y-1)^2 + \frac{3}{10M^*(\rho,y)}\lambda\rho^{\frac{5}{3}}, \end{aligned} \tag{2}$$

where the effective mass is

$$M^*(\rho,y) = \frac{M^2}{\left(M + G_{\rm S}^2\rho + 2A\rho^2 + 3B\rho^3\right)H_{\frac{5}{3}}}, \tag{3}$$

with $H_{\frac{5}{3}} = 2^{\frac{2}{3}}[y^{\frac{5}{3}} + (1-y)^{\frac{5}{3}}]$, $\lambda = (3\pi^2/2)^{\frac{2}{3}}$, and $y = \rho_p/\rho$ being the proton fraction of the system. The proton density is ρ_p. For a detailed derivation of Eq. (2) from Eq. (1) in the $y = 1/2$ case, we refer the reader to Ref. [24].

The coupling constants of the model are $G_{\rm S}^2$, $G_{\rm V}^2$, A, B, and $G_{\rm TV}^2$. The first four of them are adjusted in order to fix ρ_o, B_o, K_o, and M_o^*. This is done by solving a system of four equations, namely, $\varepsilon^{\rm (NR)}(\rho_o,1/2) = -B_o$, $K^{\rm (NR)}(\rho_o,1/2) = K_o$, $P^{\rm (NR)}(\rho_o,1/2) = 0$ (nuclear matter saturation), and $M^*(\rho_o,1/2) = M_o^*$. The pressure and incompressibility are defined, respectively, by $P^{\rm (NR)}(\rho,y) = \rho^2\frac{\partial(\varepsilon^{\rm (NR)}/\rho)}{\partial\rho}$ and $K^{\rm (NR)}(\rho,y) = 9\frac{\partial P^{\rm (NR)}}{\partial\rho}$.

An advantage of this approach is that we can obtain simple analytical expressions for the equations of state (EOS) of the model, in comparison to those calculated in the exact FR models. It is worth mentioning that in the EOS of the NR limit of the NLPC models, there are no quantities found in a self-consistent way. All observables are functions of ρ and y, as one can see, for instance, in Eq. (2). Thus, the study of the correlation between the symmetry energy and its slope can be performed analytically. For this purpose, we first use Eq. (2) to write $\mathcal{S}(\rho) = \frac{1}{8}[\frac{\partial^2(\varepsilon^{\rm (NR)}/\rho)}{\partial y^2}]_{y=\frac{1}{2}}$. Then, $J = \mathcal{S}(\rho_o)$ is given by

$$J = \frac{\lambda\rho_o^{\frac{2}{3}}}{6M} + \left(G_{\rm S}^2 + 2A\rho_o + 3B\rho_o^2\right)\frac{\lambda\rho_o^{\frac{5}{3}}}{6M^2} + G_{\rm TV}^2\rho_o. \tag{4}$$

The symmetry energy $\mathcal{S}(\rho)$ is used again in order to obtain $L = 3\rho_o(\frac{\partial\mathcal{S}}{\partial\rho})_{\rho=\rho_o}$. The result is

$$L = \frac{\lambda\rho_o^{\frac{2}{3}}}{3M} + \left(5G_{\rm S}^2 + 16A\rho_o + 33B\rho_o^2\right)\frac{\lambda\rho_o^{\frac{5}{3}}}{6M^2} + 3G_{\rm TV}^2\rho_o. \tag{5}$$

From Eq. (4) it is possible to determine the last coupling constant $G_{\rm TV}^2$, by imposing upon the model the requirement of presenting a particular value for J.

At this point, we rewrite the coupling constants of the model, namely, $G_{\rm S}^2$, $G_{\rm V}^2$, A, and B, in terms of the bulk parameters m^*, ρ_o, B_o, and K_o. An analogous procedure is done in the context of the Skyrme models in Ref. [25] through the simulated annealing method. Therefore, it is possible to write L explicitly as $L = L(m^*,\rho_o,B_o,K_o)$. By doing so, and by subtracting $3J$ from L, we finally find a clear correlation between J and L in the following form:

$$L = 3J + f(m^*,\rho_o,B_o,K_o), \tag{6}$$

where the function

$$f(m^*,\rho_o,B_o,K_o) = \left(\frac{1}{m^*} - 1\right)g(\rho_o) + h(\rho_o,B_o,K_o) \tag{7}$$

exhibits a dependence on the inverse of the effective mass. The functions $g(\rho_o)$ and $h(B_o,K_o,\rho_o)$ are written, respectively,

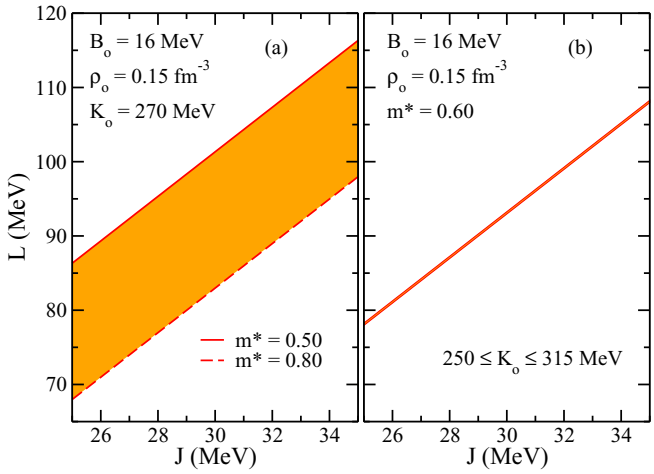

FIG. 1. (Color online) Effect of Δf in the L-J correlation of Eq. (6) for (a) $0.50 \leqslant m^* \leqslant 0.80$ and (b) $250 \leqslant K_o \leqslant 315$ MeV.

as

$$g(\rho_o) = \frac{\lambda \rho_o^{\frac{2}{3}}}{3M}\left[1 + \frac{2E_{\rm F}^o}{\left(M - 2E_{\rm F}^o\right)} - \frac{\left(M - 10E_{\rm F}^o\right)ME_{\rm F}^o}{\left(3M^2 - 19E_{\rm F}^oM + 18E_{\rm F}^{o2}\right)\left(M - 2E_{\rm F}^o\right)}\right] \quad (8)$$

and

$$h(\rho_o, B_o, K_o) = -\frac{\lambda \rho_o^{\frac{2}{3}}}{6M}\left[1 + \frac{2E_{\rm F}^o\left(M - 9E_{\rm F}^o - 27B_o\right) + K_oM}{\left(3M^2 - 19E_{\rm F}^oM + 18E_{\rm F}^{o2}\right)}\right], \quad (9)$$

with $E_{\rm F}^o = 3\lambda\rho_o^{\frac{2}{3}}/10M$. Equations (6)–(9) contain the main result of our paper. They show, in an analytical way, a linear correlation between L and J. Moreover, if we keep fixed the values ρ_o, B_o, and K_o, the functions $g(\rho_o)$ and $h(\rho_o, B_o, K_o)$ become constant. Therefore, Eq. (6) will exhibit parallel lines for different m^* values [see Fig. 1(a)].

Usually, in nuclear mean-field models, the binding energy and the saturation density are well established closely around the values of $B_o = 16$ MeV and $\rho_o = 0.15$ fm^{-3}. The same assumption does not apply to the incompressibility and effective mass. Therefore, it is important to see how the function $f(m^*, \rho_o, B_o, K_o)$ in Eq. (7) varies as a function of K_o, or of m^* for the mentioned values of B_o and ρ_o. From Eqs. (7)–(9), it is straightforward to check that, for a fixed value of m^*, the variation in f will be given by

$$(\Delta f)_{K_o} = -\frac{\lambda\rho_o^{\frac{2}{3}}}{18M^2 - 114E_{\rm F}^oM + 108E_{\rm F}^{o2}}\Delta K_o. \quad (10)$$

For the range of $250 \leqslant K_o \leqslant 315$ MeV, recently proposed in Ref. [26], one can verify that $|(\Delta f)_{K_o}| = 0.32$ MeV. On the other hand, by choosing two different models presenting the same incompressibility K_o but with two different effective masses m_1^* and m_2^*, the f variation can be inferred by

$$(\Delta f)_{m^*} = -\frac{g(\rho_o)}{m_1^*m_2^*}\Delta m^*, \quad (11)$$

where $\Delta m^* = m_2^* - m_1^*$. For a typical range of $0.50 \leqslant m^* \leqslant 0.80$, presented by FR-RMF models, one has $|(\Delta f)_{m^*}| = 18$ MeV, since $g(\rho_o = 0.15\ \text{fm}^{-3}) = 24.5$ MeV.

Figure 1 shows how such variations affect the correlation given in Eq. (6). From this figure we can conclude that different models presenting the same effective mass will exhibit points on a $L \times J$ graph situated very close to the same line, since in this case the variation of the linear coefficient in Eq. (6) is very small compared to that of the case in which K_o is fixed. This leads us to draw the conclusion that, in the NR limit of the NLPC models described by Eq. (1), the linear correlation between J and L in Eq. (6) is achieved for the more distinct models under the condition that their effective masses are equal. Before we end this section, let us remark that in Refs. [8,9] the authors could have anticipated a $J \times L$ correlation if they had worked out their general results for $L(\rho = \rho_o)$ and $E_{\rm sym}(\rho = \rho_o)$. Regarding this correlation itself, let us emphasize here that, mathematically, the linear behavior is ensured in the NR limit of the NLPC model, since there is only one isovector parameter, namely, $G_{\rm TV}^2$, in the equations of J and L [see Eqs. (4) and (5)]. Thus, the result pointed out in Eq. (6) reflects the limitation of the model parameters, in particular, the isovector one. We defer to a future work on further investigations of possible, not necessarily linear, analytical correlations between J and L for models with more than one isovector parameter.

III. PREDICTIONS OF FR-RMF MODELS

A. Symmetry energy slope

Now, we pose the question of whether the NR correlation obtained in Eq. (6) and the results showed in Fig. 1 with the subsequent conclusions still remain valid for exact FR models. The answer is given by the study we have done for a set of representative FR models, whose results are displayed in Fig. 2.

Figure 2(a) shows the J dependence on L for three different parametrizations of the FR models. For each one of them, we kept fixed their respective bulk parameters m^*, ρ_o, B_o, and K_o, but we allowed their symmetry energy J to vary. One can verify that, for each value of J, the corresponding L, obtained from the relativistic FR models calculations, will be a point on a line of angular coefficient equal to 3. Furthermore, it is also observed that L decreases as m^* increases, which is exactly the same result found in the NR limit. In Fig. 2(b), we selected a set of FR parametrizations [12,27–35], presenting the same effective mass, in this case $m^* = 0.60$. A best-fitting curve for these points indicates a line, as was also indicated by the NR calculations. Moreover, its angular coefficient is given by 2.96, which is practically the same number found in Eq. (6). For a complete list of the FR-RMF models used in this work with their main saturation properties, we refer the reader to the Appendix.

As an application of the J-L correlation found in this work, we furnish a constraint under the values of L for the

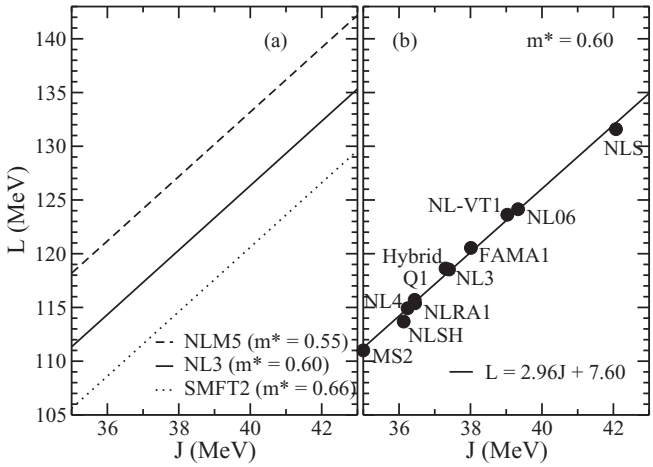

FIG. 2. L vs J for the (a) NLM5 [36], NL3 [27], and SMFT2 [37] FR parametrizations (see text) and (b) FR parametrizations in which m^* is the same.

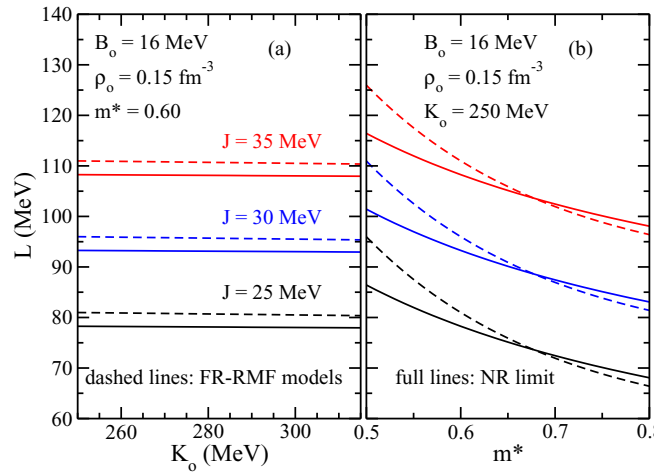

FIG. 4. (Color online) Comparison between the (a) K_o and (b) m^* dependencies of L for NR and FR-RMF models at $J = 25$, 30, and 35 MeV.

Boguta-Bodmer FR models. In order to do that, we first restrict the range of effective masses to those of the FRS constraint. Following Ref. [6], we find that this is the range of m^* in which Boguta-Bodmer models have to be constrained in order to produce spin-orbit splittings in agreement with well-established experimental values for ^{16}O, ^{40}Ca, and ^{208}Pb. By having this constraint as a starting point, we can construct a limiting line defined by $m^* = 0.58$ and another one at $m^* = 0.64$ in the $L \times J$ plane. We have constructed such lines for the same FR models as in Fig. 2(b) by keeping their ρ_o, B_o and K_o values but changing their effective mass for $m^* = 0.58$ and $m^* = 0.64$. The result is shown in Fig. 3. Notice that the correlation we have found, together with the range for the effective mass obtained in Ref. [6], naturally establishes a band of possible values of L as a function of J for the Boguta-Bodmer models. In the figure, we show this band in the particular range of $25 \leqslant J \leqslant 35$ MeV.

In order to test whether the FR-RMF models satisfy this constraint, we included in the inset of Fig. 3 some FR parametrizations compatible with the FRS constraint, namely, the same of Fig. 2(b) together with CS [38], E [38], ER [38], NL3* [39], NLB [40], NLB1 [23], NLC [40], NLRA [41], NLZ [34], NLZ2 [34], and VT [38]. We see that all of them fall inside the band.

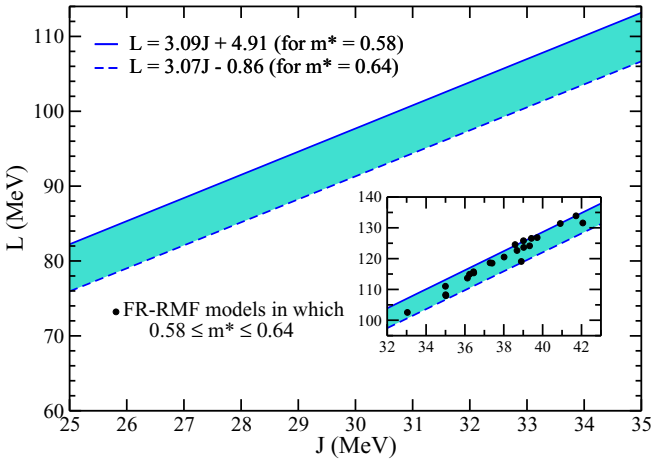

FIG. 3. (Color online) Graphic constraint in the $L \times J$ plane (see text).

Before we end this section we remark here that the NR limit also predicts, for a fixed value of J, correlations between L and the quantities K_o and m^*, according to Eqs. (6)–(9). For constant m^*, L scales as $-K_o$, while for constant K_o, L scales as $1/m^*$. In Fig. 4, we show such dependencies for NR models as well as for the FR-RMF ones.

As we can see, both approaches present the same L variation tendency regarding K_o and m^*. Notice also that, as m^* increases, in the case of K_o fixed [Fig. 4(b)], the NR limit better approaches the exact FR-RMF models.

B. Symmetry energy curvature

In the NR framework it is also possible to find an analytical expression for $K_{\rm sym} = 9\rho_o^2(\frac{\partial^2 \mathcal{S}}{\partial \rho^2})_{\rho=\rho_o}$. It reads

$$K_{\rm sym} = \left(\frac{1}{m^*} - 1\right) s(\rho_o) + r(\rho_o, B_o, K_o) \tag{12}$$

with

$$s(\rho_o) = \frac{5\lambda \rho_o^{\frac{2}{3}}}{3M}\left[1 + \frac{4E_{\rm F}^o}{(M - 2E_{\rm F}^o)} - \frac{E_{\rm F}^o(M - 10E_{\rm F}^o)(19M - 18E_{\rm F}^o)}{5(M - 2E_{\rm F}^o)(3M^2 - 19E_{\rm F}^o M + 18E_{\rm F}^{o2})}\right] \tag{13}$$

and

$$r(\rho_o, B_o, K_o) = -\frac{\lambda \rho_o^{\frac{2}{3}}}{3M}\left[1 + \frac{K_o(19M - 18E_{\rm F}^o)}{2(3M^2 - 19E_{\rm F}^o M + 18E_{\rm F}^{o2})} - \frac{(81B_o M + 8E_{\rm F}^o M + 18E_{\rm F}^{o2})}{3M^2 - 19E_{\rm F}^o M + 18E_{\rm F}^{o2}}\right]. \tag{14}$$

By rearranging these equations, we find a simplified form for $K_{\rm sym}$, namely,

$$K_{\rm sym} = [L - 3J]p(\rho_o) + q(\rho_o, B_o, K_o), \tag{15}$$

where

$$p(\rho_o) = \frac{s(\rho_o)}{g(\rho_o)} \tag{16}$$

and

$$\begin{aligned} q(\rho_o, B_o, K_o) &= -h(\rho_o, B_o, K_o)p(\rho_o) + r(\rho_o, B_o, K_o) \\ &= \frac{\lambda\rho_o^{\frac{2}{3}}}{3M}\left\{\frac{[p(\rho_o)-2]}{2} + \frac{ME_{\rm F}^o[p(\rho_o)+8]}{\left(3M^2 - 19E_{\rm F}^oM + 18E_{\rm F}^{o2}\right)}\right. \\ &\quad - \frac{9E_{\rm F}^{o2}[p(\rho_o)-2] + 27B_o\left[E_{\rm F}^o p(\rho_o) - 3M\right]}{\left(3M^2 - 19E_{\rm F}^oM + 18E_{\rm F}^{o2}\right)} \\ &\quad \left. + \frac{M[p(\rho_o)-19] + 18E_{\rm F}^o}{2\left(3M^2 - 19E_{\rm F}^oM + 18E_{\rm F}^{o2}\right)}K_o\right\}. \end{aligned} \tag{17}$$

In the above, $p(\rho_o) = 5.13$ at $\rho_o = 0.15$ fm^{-3} and an L and J dependence of $K_{\rm sym}$ is explicit [see Eq. (15)]. It is worth noting that the mathematical relation presented between $K_{\rm sym}$ and L was based on the result of Eq. (6), which by itself is a consequence of the limitation of the number of isovector parameters of the NR limit of the NLPC model, in this case only one, $G_{\rm TV}^2$. For models with two or more isovector parameters, the correlation between J and L and, consequently, the other between $K_{\rm sym}$ and L (or between $K_{\rm sym}$ and J) may follow a behavior different from the linear one.

Once again, we test whether these results reflect the FR-RMF model calculations. First, notice that Eq. (12) predicts constant $K_{\rm sym}$ for fixed values of K_o and m^*, quite independent of J. For the sake of illustration we calculate $K_{\rm sym}$ for a set of FR-RMF models with $\rho_o = 0.15$ fm^{-3}, $B_o = 16$ MeV, $K_o = 270$ MeV, and $m^* = 0.60$, with J running in the range of $25 \leqslant J \leqslant 35$ MeV. For these cases, we have obtained a unique value of $K_{\rm sym} = 96.4$ MeV, supporting the NR prediction of Eq. (12).

Still analyzing Eq. (12), we can see that a variation in m^* produces a spread in $K_{\rm sym}$ of

$$\Delta K_{\rm sym} = -\frac{s(\rho_o)}{m_1^* m_2^*}\Delta m^*, \tag{18}$$

for K_o fixed. Thus, the range of m^* given by the FRS constraint generates $|\Delta K_{\rm sym}| = 20$ MeV, since $s(\rho_o = 0.15$ fm$^{-3}) = 125.7$ MeV. A non-negligible spread in $K_{\rm sym}$ is also observed for models with constant m^* and different K_o. For such cases, one can see that this spread is entirely due to

$$\Delta r = -\frac{\lambda\rho_o^{\frac{2}{3}}\left(19M - 18E_{\rm F}^o\right)}{18M^3 - 114E_{\rm F}^oM^2 + 108ME_{\rm F}^{o2}}\Delta K_o. \tag{19}$$

For the range of $250 \leqslant K_o \leqslant 315$ MeV, we calculate $|\Delta K_{\rm sym}| = 5.9$ MeV.

Based on this study and Eq. (15), we can conclude, for instance, that the linear correlation between $K_{\rm sym}$ and L for constant J will certainly occur for models in which $\Delta r = 0$, i.e., for fixed K_o. We verified this prediction for the FR-RMF models of Ref. [14] with $J = 32.5$ MeV and $K_o = 230$ MeV. The result is depicted in Fig. 5(a).

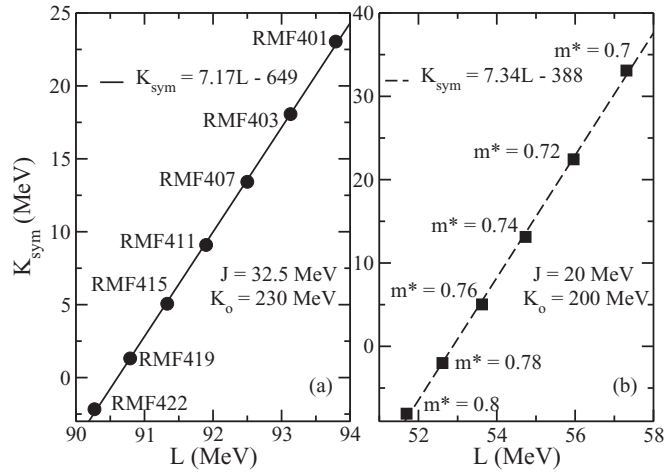

FIG. 5. Correlation between $K_{\rm sym}$ and L (see text).

The figure clearly confirms the prediction of Eq. (15). Even the angular coefficient, 7.17, is comparable with the value $p(\rho_o) = 5.13$ (at $\rho_o = 0.15$ fm^{-3}) of the NR calculation.

We remark here that the correlation observed in Fig. 5(a) only occurs for models with the same values for K_o and J (230 and 32.5 MeV, respectively, in this case). If J is not the same, $K_{\rm sym}$ will be random and independent of the value of L. Indeed, most FR-RMF models in the literature can suggest that $K_{\rm sym}$ first decreases with the increase of L and attains a minimum at about $L = 70$ MeV, then rises back for larger L. We reinforce that our study indicates that, in the Boguta-Bodmer models, such analysis must take into account the values of K_o and J of the parametrization, in the sense that only with these values fixed will the linear correlation between $K_{\rm sym}$ and L be established. In order to show that $K_{\rm sym} \propto L$ even for parametrizations presenting $L < 70$ MeV, we have constructed Boguta-Bodmer models with fixed bulk parameters $\rho_o = 0.15$ fm^{-3}, $B_o = 16$ MeV, $K_o = 200$ MeV, and $J = 20$ MeV, and with m^* in the range of $0.7 \leqslant m^* \leqslant 0.8$. In such a case, the parametrizations present $L < 70$ MeV, and one can see from Fig. 5(b) that the linear correlation between $K_{\rm sym}$ and L is preserved. Notice, however, that, as the value $J = 20$ MeV is actually ruled out by experimental evidences, our analysis suggests that despite being mathematically valid for $L < 70$ MeV, the correlation between $K_{\rm sym}$ and L for Boguta-Bodmer models predicts higher values for the symmetry energy slope [see Fig. 5(a)]. This is a direct consequence of the model structure itself, regarding the number of free isovector parameters. Indeed, the prediction of higher L values for acceptable J values can also be seen in Fig. 3.

For the sake of completeness, we use the correlations among the symmetry energy, its slope, and curvature to propose another graphic constraint in the $K_{\rm sym} \times L$ plane that FR-RMF models must satisfy. For this purpose, we used the relativistic framework to construct boundaries in that plane by observing the FRS constraint and the ranges of $250 \leqslant K_o \leqslant 315$ MeV

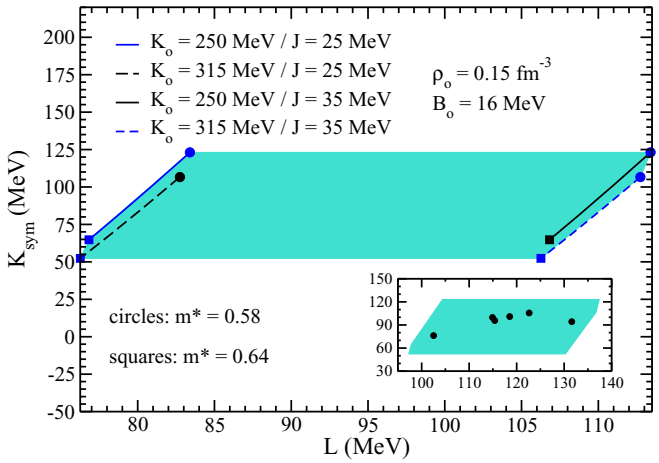

FIG. 6. (Color online) Graphic constraint in the $K_{\rm sym}\times L$ plane (see text).

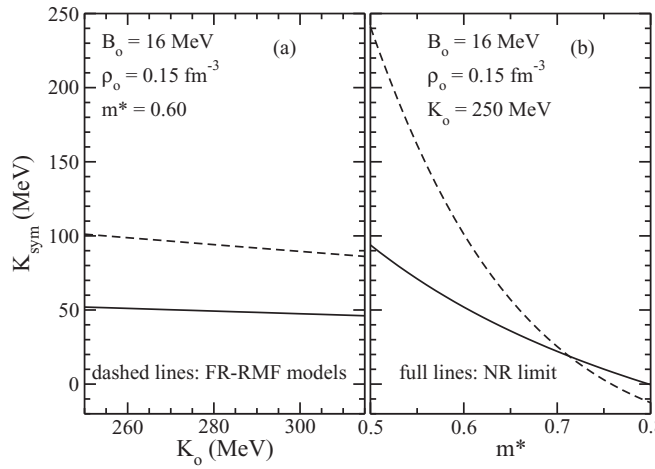

FIG. 7. Comparison between the (a) K_o and (b) m^* dependencies of $K_{\rm sym}$ for NR and FR-RMF models.

and $25 \leqslant J \leqslant 35$ MeV. Within such boundaries, we have fixed the values of $\rho_o = 0.15$ fm^{-3} and $B_o = 16$ MeV. This procedure leads to the band shown in Fig. 6; i.e., all FR-RMF models presenting m^*, K_o, and J in the mentioned ranges must produce points on the $K_{\rm sym}\times L$ graph inside this band. In order to test this prediction, we selected the same FR-RMF parametrizations of the inset of Fig. 3, which presents $250 \leqslant K_o \leqslant 315$ MeV and the reconstructed the band in the $K_{\rm sym}\times L$ plane to take into account that such models have $32 \leqslant J \leqslant 43$ MeV (see the inset of Fig. 3). The new band is represented in the inset of Fig. 6. We can see that all FR-RMF models (NL3*, NLS, NL4, NL3, NLB1, and NLRA1), represented by the full circles, fall inside the band. In the next section we discuss this correlation in a more critical way.

As a last remark, we proceed to show the K_o and m^* dependence of $K_{\rm sym}$ by using Eq. (12). Notice that, exactly as in the case of the symmetry energy slope, Eq. (12) expresses clear correlations of $K_{\rm sym}$ with the incompressibility and effective mass, namely, $K_{\rm sym} \sim -K_o$ and $K_{\rm sym} \sim 1/m^*$ for fixed values of m^* or K_o, respectively. This behavior is depicted in Fig. 7, which also shows a direct comparison between the results for the NR and FR-RMF approaches.

As in the case of the symmetry energy slope, we see that, as m^* increases, $K_{\rm sym}$ decreases, while, for both NR and FR-RMF, the K_o dependence of $K_{\rm sym}$ is very weak compared to the m^* one.

IV. SUMMARY AND CONCLUSION

Since, in the majority of RMF models, B_o and ρ_o are chosen to be very close to 16 MeV and 0.15 fm^{-3}, respectively, in this section, we will forget such model dependence on them. Here, we are concerned with the m^* and K_o dependencies.

In summary, the study performed in this paper indicates that the nonrelativistic limit of the NLPC models described by Eq. (1) can be used as a suitable guideline to infer possible correlations related to the FR relativistic models with σ^3 and σ^4 self-interactions. Regarding the correlations between the quantities at the saturation density ($\rho = \rho_o$), obtained from the nonrelativistic limit and reproduced by the FR relativistic models, our main findings are the following:

(i) In the NR approximation, the symmetry energy slope L is linearly correlated with J [see Eq. (6)]. Moreover, this same equation shows that L also depends explicitly on the effective nucleon mass m^* [scaling as $1/m^*$; see Eqs. (6) and (7)] and the incompressibility K_o [scaling linearly; see Eqs. (6)–(9)]. The K_o dependence of L has been verified to be negligible, as shown by the full lines of Fig. 4(a). We verified that the same features are also found in the FR-RMF Boguta-Bodmer models, as one can see in Fig. 2 and in the dashed lines of Fig. 4.

(ii) The symmetry energy curvature $K_{\rm sym}$ depends on m^*, scaling as $1/m^*$, and is linearly correlated with K_o in the NR approach [see Eqs. (12)–(14)]. Such dependencies are not negligible. By aiming at finding an L (or J) dependence in $K_{\rm sym}$, we have rewritten $K_{\rm sym}$ as presented in Eq. (15): $K_{\rm sym} = [L - 3J]p(\rho_o) + q(\rho_o, B_o, K_o)$. However, the existing correlation between L and J [see Eq. (6)] shows that, for a fixed value of K_o, there are two possible scenarios, namely, (i) a linear correlation between $K_{\rm sym}$ and L for models in which J is the same and (ii) a linear correlation between $K_{\rm sym}$ and J for models in which L is the same. Once again, the same correlations also apply to the FR-RMF Boguta-Bodmer models, as displayed in Figs. 7 and 5.

(iii) Convinced of the correlation between L and J, found in the NR approximation and confirmed for the relativistic calculations, we have constructed a region of possible L values as a function of J and according to the FRS constraint [6] that FR-RMF Boguta-Bodmer models must satisfy in order to give values for the finite nuclei spin-orbit splitting compatible with well-established experimental values (see Fig. 3).

(iv) In Fig. 8, we present our prediction for the lowest and highest values for L in comparison with other values found in the literature, by taking into account

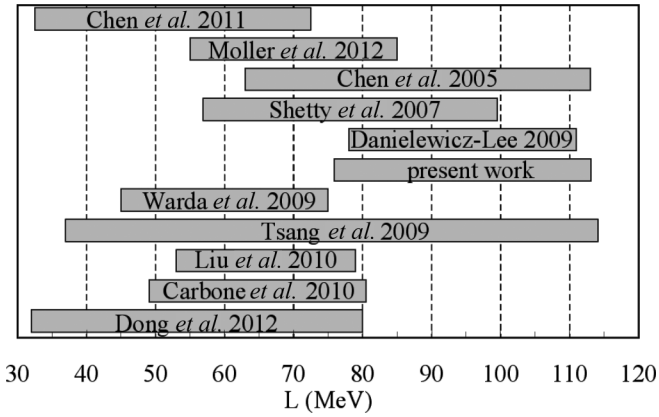

FIG. 8. Comparison between the limits of L obtained in this work and those from Dong *et al.* [42], Carbone *et al.* [43], Liu *et al.* [44], Tsang *et al.* [45], Warda *et al.* [46], Danielewicz and Lee [47], Shetty *et al.* [48], Chen *et al.* [49], Möller *et al.* [50], and Chen [51].

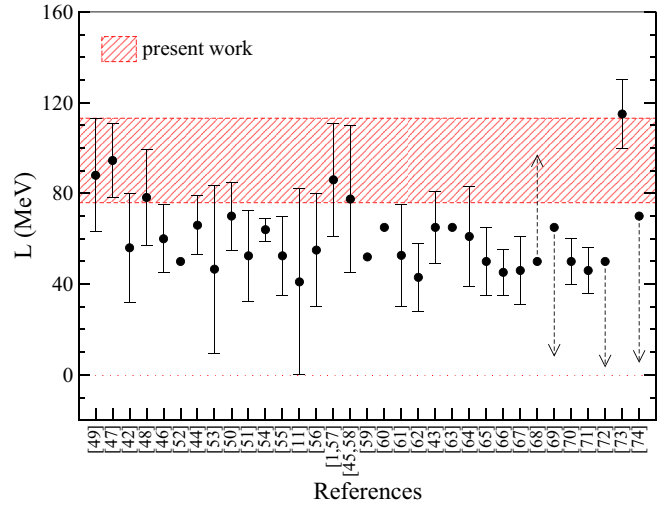

FIG. 9. (Color online) Comparison between the limits of L obtained in this work and those from 33 different analyses of Refs. [1,11,42–74].

the region of Fig. 3 in the range of $25 \leqslant J \leqslant 35$ MeV for the symmetry energy. Notice that our limits for L are comparable with other models.

For the sake of completeness, we present in Fig. 9 a large set of L values obtained from analyses of different terrestrial nuclear experiments and astrophysical observations. They include analyses of isospin diffusion, neutron skin, pygmy dipole resonances, α and β decays, transverse flow, the mass-radius relation of neutron stars, and torsional crust oscillation of neutron stars. Twenty-eight of the 33 points shown in the figure were extracted from Table I of Ref. [75], in which the authors, through the Hugenholtz–Van Hove theorem, used these values in order to constrain the neutron-proton effective mass splitting in nonrelativistic nuclear models.

(v) Analogously, but based on the situation in which the correlation between $K_{\rm sym}$ and L is achieved, we have also proposed a graphic constraint in the $K_{\rm sym} \times L$ plane that the FR-RMF models at the FRS condition and presenting $25 \leqslant J \leqslant 35$ MeV must obey (see Fig. 6).

Before we end this work, some words of caution are needed. First, we have studied a particular class of $\sigma^3 + \sigma^4$ self-interaction RMF models where the nonrelativistic limit used a point-coupling approximation of them. Nevertheless, what we have called exact calculations in this work have no other approximation than that of the mean field, and the point-coupling versions of them are absent. Second, our cautionary words here are more in the sense that, nowadays, of the several families of RMF models (for a review, see, for instance, Ref. [76]), some of which are density dependent, not all will necessarily follow the same features of the FR-RMF models studied here.

ACKNOWLEDGMENTS

We are grateful for partial support from Fundação de Amparo à Pesquisa do Estado de São Paulo (FAPESP) and Coordenação de Aperfeiçoamento de Pessoal de Nível Superior (CAPES) of Brazil.

APPENDIX: SATURATION PROPERTIES OF THE FR-RMF MODELS

In this Appendix we show in Table I the mainly saturation properties, calculated at the saturation density, of the FR-RMF models used in our work.

TABLE I. Nuclear matter properties, at the saturation density, of the FR-RMF models used in this work.

Model	ρ_o (fm^{-3})	B_o (MeV)	K_o (MeV)	m^*	J (MeV)	L (MeV)	$K_{\rm sym}$ (MeV)
CS	0.150	16.17	187.21	0.58	40.91	131.42	136.68
E	0.150	16.13	221.43	0.58	38.58	124.57	132.12
ER	0.149	16.16	220.49	0.58	39.42	126.60	127.62
FAMA1	0.148	16.00	200.05	0.60	38.01	120.53	113.22
Hybrid	0.148	16.24	230.01	0.60	37.30	118.62	110.94
MS2	0.148	15.75	249.92	0.60	35.00	111.00	100.85
NL-VT1	0.150	16.09	179.03	0.60	39.03	123.63	117.72
NL06	0.147	16.05	195.09	0.60	39.33	124.14	110.85
NL3	0.148	16.24	271.53	0.60	37.40	118.53	100.88

TABLE I. (*Continued.*)

Model	ρ_o (fm^{-3})	B_o (MeV)	K_o (MeV)	m^*	J (MeV)	L (MeV)	K_{sym} (MeV)
NL3*	0.150	16.31	258.25	0.59	38.68	122.63	105.56
NL4	0.148	16.16	270.34	0.60	36.24	114.92	99.72
NLB	0.148	15.77	421.02	0.61	35.01	108.26	54.94
NLB1	0.162	15.79	280.44	0.62	33.04	102.51	76.15
NLC	0.148	15.77	224.46	0.63	35.02	107.97	76.91
NLM5	0.160	16.00	200.00	0.55	30.00	103.18	179.44
NLRA	0.157	16.25	320.48	0.63	38.90	119.09	62.11
NLRA1	0.147	16.15	285.23	0.60	36.45	115.38	95.72
NLS	0.150	16.44	262.94	0.60	42.07	131.59	94.22
NLSH	0.146	16.36	355.65	0.60	36.13	113.68	79.83
NLZ	0.151	16.18	172.84	0.58	41.72	133.91	140.19
NLZ2	0.151	16.06	172.23	0.58	39.01	125.82	140.62
Q1	0.148	16.10	241.86	0.60	36.44	115.71	105.65
RMF401	0.153	16.30	229.99	0.71	32.50	93.79	23.04
RMF403	0.153	16.30	229.99	0.72	32.50	93.13	18.06
RMF407	0.153	16.30	229.99	0.73	32.50	92.50	13.42
RMF411	0.153	16.30	229.99	0.74	32.50	91.90	9.09
RMF415	0.153	16.30	229.98	0.75	32.50	91.33	5.06
RMF419	0.153	16.30	229.99	0.76	32.50	90.79	1.31
RMF422	0.153	16.30	229.99	0.77	32.50	90.27	−2.17
SMFT2	0.162	13.78	211.31	0.66	17.38	52.73	60.27
VT	0.153	16.09	172.74	0.59	39.72	126.83	130.05

[1] L. W. Chen, C. M. Ko, and B. A. Li, Phys. Rev. Lett. **94**, 032701 (2005).
[2] M. Dutra, O. Lourenço, J. S. Sá Martins, A. Delfino, J. R. Stone, and P. D. Stevenson, Phys. Rev. C **85**, 035201 (2012).
[3] L. L. Lopes and D. P. Menezes, arXiv:1405.5259v1.
[4] A. Delfino, T. Frederico, V. S. Timóteo, and L. Tomio, Phys. Lett. B **634**, 185 (2006).
[5] F. Coester, S. Cohen, B. D. Day, and C. M. Vincent, Phys. Rev. C **1**, 769 (1970).
[6] R. J. Furnstahl, J. J. Rusnak, and B. D. Serot, Nucl. Phys. A **632**, 607 (1998).
[7] C. Ducoin, J. Margueron, C. Providência, and I. Vidaña, Phys. Rev. C **83**, 045810 (2011).
[8] R. Chen, B. J. Cai, L. W. Chen, B. A. Li, X. H. Li, and C. Xu, Phys. Rev. C **85**, 024305 (2012).
[9] B. J. Cai and L. W. Chen, Phys. Lett. B **711**, 104 (2012).
[10] J. R. Stone and P. G. Reinhard, Prog. Nucl. Phys. **58**, 587 (2007).
[11] L. W. Chen, C. M. Ko, B.-A. Li, and J. Xu, Phys. Rev. C **82**, 024321 (2010).
[12] J. Piekarewicz, Phys. Rev. C **66**, 034305 (2002).
[13] N. K. Glendenning, *Compact Stars: Nuclear Physics, Particle Physics, and General Relativity*, 2nd ed. (Springer, New York, 2000).
[14] A. A. Dadi, Phys. Rev. C **82**, 025203 (2010).
[15] J. Boguta and A. R. Bodmer, Nucl. Phys. A **292**, 413 (1977).
[16] J. J. Rusnak and R. J. Furnstahl, Nucl. Phys. A **627**, 495 (1997).
[17] D. G. Madland, T. J. Bürvenich, J. A. Maruhn, and P.-G. Reinhard, Nucl. Phys. A **741**, 52 (2004).
[18] O. Lourenço, M. Dutra, R. L. P. G. Amaral, and A. Delfino, Braz. J. Phys. **42**, 227 (2012); O. Lourenço, M. Dutra, A. Delfino, and R. L. P. G. Amaral, Int. J. Mod. Phys. E **16**, 3037 (2007).
[19] P. W. Zhao, Z. P. Li, J. M. Yao, and J. Meng, Phys. Rev. C **82**, 054319 (2010).
[20] T. Niksic, D. Vretenar, and P. Ring, Prog. Part. Nucl. Phys. **66**, 519 (2011).
[21] B. A. Nikolaus, T. Hoch, and D. G. Madland, Phys. Rev. C **46**, 1757 (1992).
[22] G. Gelmini and B. Ritzi, Phys. Lett. B **357**, 431 (1995); A. Delfino, M. Malheiro, and T. Frederico, Braz. J. Phys. **31**, 518 (2001).
[23] P.-G. Reinhard, Rep. Prog. Phys. **52**, 439 (1989).
[24] O. Lourenço, M. Dutra, A. Delfino, and J. S. Sá Martins, Phys. Rev. C **81**, 038201 (2010).
[25] B. K. Agrawal, S. Shlomo, and V. K. Au, Phys. Rev. C **72**, 014310 (2005).
[26] J. R. Stone, N. J. Stone, and S. A. Moszkowski, Phys. Rev. C **89**, 044316 (2014).
[27] G. A. Lalazissis, J. König, and P. Ring, Phys. Rev. C **55**, 540 (1997).
[28] H. Müller and B. D. Serot, Nucl. Phys. A **606**, 508 (1996).
[29] B. Nerlo-Pomorska and J. Sykut, Int. J. Mod. Phys. E **13**, 75 (2004).
[30] M. Rashdan, Phys. Rev. C **63**, 044303 (2001).
[31] R. J. Furnstahl, B. D. Serot, and H. B. Tang, Nucl. Phys. A **615**, 441 (1997).
[32] J. Piekarewicz and M. Centelles, Phys. Rev. C **79**, 054311 (2009).
[33] Internal discussion notes, ORNL, U. Erlangen, U. Frankfurt, U. T. Knoxville, U. Oxford, Vanderbilt and U. Warsaw (private communication).
[34] M. Bender, K. Rutz, P.-G. Reinhard, J. A. Maruhn, and W. Greiner, Phys. Rev. C **60**, 034304 (1999).

[35] P.-G. Reinhard, Z. Phys. A **329**, 257 (1988).
[36] M. Centelles, M. D. Estal, and X. Viñas, Nucl. Phys. A **635**, 193 (1998).
[37] S. Gmuca, Z. Phys. A **342**, 387 (1992).
[38] M. Rufa, P.-G. Reinhard, J. A. Maruhn, W. Greiner, and M. R. Strayer, Phys. Rev. C **38**, 390 (1988).
[39] G. A. Lalazissis, S. Karatzikos, R. Fossion, D. Pena Arteaga, A. V. Afanasjev, and P. Ring, Phys. Lett. B **671**, 36 (2009).
[40] B. D. Serot and J. D. Walecka, Int. J. Mod. Phys. E **06**, 515 (1997).
[41] K. C. Chung, C. S. Wang, A. J. Santiago, and J. W. Zhang, Eur. Phys. J. A **9**, 453 (2000).
[42] J. Dong, W. Zuo, J. Gu, and U. Lombardo, Phys. Rev. C **85**, 034308 (2012).
[43] A. Carbone, G. Colò, A. Bracco, L.-G. Cao, P. F. Bortignon, F. Camera, and O. Wieland, Phys. Rev. C **81**, 041301(R) (2010).
[44] M. Liu, N. Wang, Z.-X. Li, and F.-S. Zhang, Phys. Rev. C **82**, 064306 (2010).
[45] M. B. Tsang, Y. Zhang, P. Danielewicz, M. Famiano, Z. Li, W. G. Lynch, and A. W. Steiner, Phys. Rev. Lett. **102**, 122701 (2009).
[46] M. Warda, X. Viñas, X. Roca-Maza, and M. Centelles, Phys. Rev. C **80**, 024316 (2009).
[47] P. Danielewicz and J. Lee, Nucl. Phys. A **818**, 36 (2009).
[48] D. V. Shetty, S. J. Yennello, and G. A. Souliotis, Phys. Rev. C **75**, 034602 (2007).
[49] L. W. Chen, C. M. Ko, and B.-A. Li, Phys. Rev. C **72**, 064309 (2005).
[50] P. Möller, W. D. Myers, H. Sagawa, and S. Yoshida, Phys. Rev. Lett. **108**, 052501 (2012).
[51] L. W. Chen, Phys. Rev. C **83**, 044308 (2011).
[52] W. D. Myers and W. J. Swiatecki, Nucl. Phys. A **601**, 141 (1996).
[53] J. M. Lattimer and Y. Lim, Astrophys. J. **771**, 51 (2013).
[54] B. K. Agrawal, J. N. De, and S. K. Samaddar, Phys. Rev. Lett. **109**, 262501 (2012).
[55] P. Danielewicz and J. Lee, Nucl. Phys. A **922**, 1 (2014).
[56] M. Centelles, X. Roca-Maza, X. Vinas, and M. Warda, Phys. Rev. Lett. **102**, 122502 (2009).
[57] B. A. Li and L. W. Chen, Phys. Rev. C **72**, 064611 (2005).
[58] M. B. Tsang *et al.*, Phys. Rev. Lett. **92**, 062701 (2004).
[59] Z. Y. Sun *et al.*, Phys. Rev. C **82**, 051603 (2010).
[60] D. V. Shetty, S. J. Yennello, and G. A. Souliotis, Phys. Rev. C **76**, 024606 (2007).
[61] C. Xu, B. A. Li, and L. W. Chen, Phys. Rev. C **82**, 054607 (2010).
[62] A. Klimkiewicz *et al.*, Phys. Rev. C **76**, 051603(R) (2007).
[63] Z. Kohley *et al.*, Phys. Rev. C **82**, 064601 (2010).
[64] J. Dong, W. Zuo, and J. Gu, Phys. Rev. C **87**, 014303 (2013).
[65] J. Dong, H. Zhang, L. Wang, and W. Zuo, Phys. Rev. C **88**, 014302 (2013).
[66] Z. Zhang and L.-W. Chen, Phys. Lett. B **726**, 234 (2013).
[67] A. Tamii, P. von Neumann-Cosel, and I. Poltoratska, Eur. Phys. J. A **50**, 28 (2014).
[68] I. Vidaña, Phys. Rev. C **85**, 045808 (2012).
[69] D. H. Wen, W. G. Newton, and B. A. Li, Phys. Rev. C **85**, 025801 (2012).
[70] A. W. Steiner, J. M. Lattimer, and E. F. Brown, Astrophys. J. **722**, 33 (2010).
[71] A. W. Steiner and S. Gandolfi, Phys. Rev. Lett. **108**, 081102 (2012).
[72] M. Gearheart, W. G. Newton, J. Hooker, and B. A. Li, Mon. Not. R. Astron. Soc. **418**, 2343 (2011).
[73] H. Sotani, K. Nakazato, K. Iida, and K. Oyamatsu, Mon. Not. R. Astron. Soc. **428**, L21 (2013).
[74] W. G. Newton and B. A. Li, Phys. Rev. C **80**, 065809 (2009).
[75] B.-A. Li and X. Han, Phys. Lett. B **727**, 276 (2013).
[76] M. Dutra, O. Lourenço, S. S. Avancini, B. V. Carlson, A. Delfino, D. P. Menezes, C. Providência, S. Typel, and J. R. Stone, arXiv:1405.3633.